Low-coherence enhanced backscattering: review of principles and applications for colon cancer screening

Young L. Kim
Vladimir M. Turzhitsky
Yang Liu
Northwestern University
Biomedical Engineering Department
Evanston, Illinois 60208

Hemant K. Roy
Ramesh K. Wali
Evanston-Northwestern Healthcare
Department of Medicine
Evanston, Illinois 60201

Hariharan Subramanian
Prabhakar Pradhan
Northwestern University
Biomedical Engineering Department
Evanston, Illinois 60208

Vadim Backman
Northwestern University
Biomedical Engineering Department
Evanston, Illinois 60208
and
Evanston-Northwestern Healthcare
Department of Medicine
Evanston, Illinois 60201

Abstract. The phenomenon of enhanced backscattering (EBS) of light, also known as coherent backscattering (CBS) of light, has been the object of intensive investigation in nonbiological media over the last two decades. However, there have been only a few attempts to explore EBS for tissue characterization and diagnosis. We have recently made progress in the EBS measurements in tissue by taking advantage of low spatial coherence illumination, which has led us to the development of low-coherence enhanced backscattering (LEBS) spectroscopy. In this work, we review the current state of research on LEBS. After a brief discussion of the basic principle of EBS and LEBS, we present an overview of the unique features of LEBS for tissue characterization, and show that LEBS enables depth-selective spectroscopic assessment of mucosal tissue. Then, we demonstrate the potential of LEBS spectroscopy for predicting the risk of colon carcinogenesis and colonoscopy-free screening for colorectal cancer (CRC).
 [DOI: 10.1117/1.2236292]

Keywords: coherent backscattering; enhanced backscattering; low coherence; elastic light scattering; spectroscopy; colorectal cancer.

Paper 05271SSR received Sep. 22, 2005; revised manuscript received Dec. 1, 2005; accepted for publication Jan. 6, 2006; published online Jul. 24, 2006.

1 Introduction

Enhanced backscattering (EBS) of light, otherwise known as coherent backscattering (CBS) of light, originates from the constructive interference in elastic light scattering, giving rise to an enhanced scattered intensity in the backward direction. For a plane wave illuminating a semi-infinite random medium, every photon scattered from the medium in the backward direction has a time-reversed photon traveling along the same path in the opposite direction, i.e., the path formed by exactly opposite sequences of the scattering centers. These photons have the same phase and thus interfere constructively with each other, resulting in an EBS peak (sometimes referred to as an EBS cone) around the backward direction. Since its first observations in aqueous suspensions,[1–3] the EBS phenomenon has been an object of intensive investigation in a variety of different systems such as strong scattering materials,[4] laser-cooled atoms,[5] liquid crystals,[6] photonic crystals,[7] amplifying materials,[8,9] and solar system bodies.[10] The EBS peak profile is further characterized by the distribution of path lengths of backscattered photons. The dependency of the profile of the EBS peak on the distribution of the path length was studied using femtosecond-resolved measurements in time domain.[11,12] EBS measurements were extended to the time-resolved phase-space distributions of the backscattered light, and it was found that for longer light paths the momentum distribution of the backscattered light was narrowed.[13] It was also shown that absorption and a finite thickness of samples removed long light paths, which made the top of the EBS peak round off.[14,15] In active random media such as random lasers, long paths were amplified and the shape of the EBS peak sharpened.[8,9] Moreover, dephasing effects, which destroy interference in the EBS phenomenon in elastic light scattering, were investigated. Faraday rotation by an external magnetic field[16,17] or a phase screw dislocation in the incident field[18] can destroy the time-reversal invariance, resulting in a distorted EBS peak. Indeed, this fascinating phenomenon has opened up a new field in classical optics, and a great amount of theoretical and experimental work already has been done in this area over the last two decades.

However, there have been only a few reports of EBS observation in biological media, and no attempt has been made to use EBS for tissue diagnosis.[19–21] Yoo et al.[19,20] first pioneered EBS in biological tissue. Yoon, Roy, and Straight[21] also used the EBS phenomenon to measure optical properties of tissue such as the transport mean free path. There is an apparent disparity between hundreds of publications dealing

Address all correspondence to Young Kim, Biomedical Engineering Department, Northwestern University, 2145 Sheridan Rd. #E310, Evanston, IL 60208; Tel: 847–491–7167; Fax: 847–491–4928; Email: younglae@northwestern.edu

1083-3668/2006/11(4)/041125/10/$22.00 © 2006 SPIE

with EBS in nonbiological media and a small number of reports on EBS for tissue characterization. The question why this fascinating effect has been underutilized in tissue optics arises, although many other optical phenomena, including elastic light scattering, fluorescence, Raman scattering, nonlinear scattering, etc., have found a plethora of applications and have been extensively used for tissue diagnosis.

The reason becomes clear if one considers the limitations that have been preventing the utilization of this otherwise remarkable optical phenomenon for biological applications. 1. Applications of conventional EBS in biological media have been hampered primarily by an extremely narrow angular width of the EBS peak ($w \approx 0.001$ deg). Because the angular width of an EBS peak is proportional to the ratio of wavelength λ of light to the transport mean free path l_s^* of light in the medium [in biological tissue, $l_s^* \approx 300$ to 2000 μm (Ref. 22)], the width of the EBS peak in tissue is very narrow, typically $w \approx 0.001$ deg (w is the angular full width at half maximum of an EBS peak). Experimental observation of such a narrow EBS peak has only recently been achieved in pioneering experiments by Sapienza et al.[6] For comparison, most EBS studies conducted to date involved nonbiological media with $l_s^* \approx 10-50$ μm (i.e., $w \approx 0.05$ to 0.3 deg) 2. Such narrow EBS peaks have been primarily used to measure l_s^* of bulk tissue, typically averaged over several cubic millimeters. However, we point out that other conventional techniques, such as diffuse reflectance measurements,[23] transmission measurements,[24] and the adding-doubling method,[25] can also determine l_s^* in random media without using the self-interference effect of the time-reversed paths. 3. Conventional EBS is masked by speckle. Ensemble averaging over hundreds of measurements or mechanical rotation of a sample is necessary to uncover an EBS peak.[21,26,27] 4. Conventional EBS does not provide spectroscopic information. So far, EBS measurements have relied on single-wavelength lasers, which do not allow spectrally resolved EBS measurements. A plethora of data has been obtained by a number of investigators showing that spectroscopic measurements of tissue optical properties are exceedingly valuable for tissue diagnosis. Thus, spectrally resolved EBS measurements are highly desirable. 5. Conventional EBS does not allow depth resolution. Because most biological tissues have multilayered structures, depth-selective measurements are crucial. However, depth-selective EBS measurements have not been achieved in tissue.

We have recently overcome all major limitations of the EBS measurements in tissue by taking advantage of low spatial coherence illimination.[28–30] The finite spatial coherence length of illumination dephases the conjugated time-reversed waves outside its spatial coherence area. As discussed later, such low-coherence EBS (LEBS) significantly simplifies EBS observation in tissue, offering several critical advantages such as speckle reduction, dramatic broadening of the EBS peak, sensitivity to low-order scattering, and depth-selective measurements of tissue properties. Investigation of LEBS is further underscored by our demonstration that LEBS spectroscopy can be used to detect early precancerous alterations in the colon far earlier than is currently feasible by means of any available histological, molecular, and even genetic technique.[28–31]

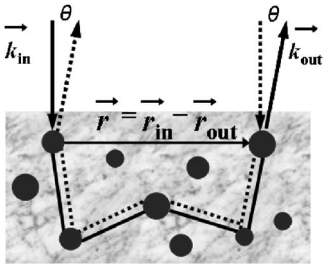

Fig. 1 Illustration of the EBS phenomenon. EBS originates from the constructive interference between pairs of photons propagating along a scattering light path (solid arrows) and its time-reversed path (dashed arrows) in the case when the photons exit the medium in directions close to the backscattering ($\theta \rightarrow 0$ deg). When both waves emerge from the medium, they have an identical phase. Thus, they interfere constructively with each other, resulting in an enhanced scattered intensity in the backward direction.

In this work, we review recent progress in the understanding of the mechanism of the LEBS phenomenon and its applications for colon cancer detection and screening. First, we provide an overview of basic principles of EBS and LEBS. In Sec. 2, we introduce the basic principle of EBS and LEBS. In Sec. 3, we present the experimental setup of LEBS spectroscopy and discuss LEBS advantages over conventional EBS. Finally, in Sec. 4, we report animal and pilot human studies that demonstrate the potential of LEBS for colon cancer detection and screening.

2 Background

2.1 *Principles of Enhanced Backscattering*

For a plane wave illuminating a semi-infinite random medium, every photon scattered from the medium in the backward direction has a time-reversed photon traveling along the same path in the opposite direction, i.e., the paths formed by exactly opposite sequences of scattering centers. The phase difference between these two waves following the identical path in time-reversed order is $\Delta\varphi = (\kappa_{in} + \kappa_{out}) \cdot (r_{in} - r_{out})$, as shown in Fig. 1. The phase difference must be sufficiently small for constructive interference to occur. For backscattered light, $\kappa_{in} + \kappa_{out} \rightarrow 0$, the phase difference becomes very small, and thus, the two waves following the time-reversed paths interfere with each other constructively. This constructive interference occurs in the backscattering direction, whereas in directions sufficiently away from the backward direction, the constructive interference vanishes. In principle, the peak EBS intensity can be twice as high as the incoherent intensity scattered outside the EBS peak (in EBS literature, this intensity is frequently referred to as the "background intensity").

The EBS phenomenon can be understood in the context of Young's double pinhole interference experiment. Conceptually, the first and last scatterers in EBS can be considered the double pinholes in the Young's double pinhole experiment. A plane wave passing the double pinholes produces a sinusoidal fringe pattern in the far field. Its maximum intensity is formed at $\theta = 0$ deg and its fringe spacing is inversely proportional to the distance between the pinholes. Similarly, in EBS a plane wave passing the first and last scatterers through the time-reversed paths would produce a sinusoidal fringe pattern with

its maximum intensity in the backward direction. Its fringe spacing is inversely proportional to the transverse distance between the first and last scatterers. In EBS, all possible transverse distances between the first and last scatterers average out the fringe patterns except the backward direction, resulting in an enhanced peak. Therefore, the width of the enhanced peak is primarily dependent on the average distance between the first and last scatterers [i.e., the transport mean free path $l_s^*=l_s/(1-g)$, where l_s is the scattering mean free path and g is the anisotropy factor], such that the full width half maximum (FWHM) of the EBS peak in a semi-infinite disordered medium $w\approx\lambda/(3\pi l_s^*)\approx 0.7/(\kappa l_s^*)$, where λ and κ are the wavelength and wavevector of light, respectively. Thus, in conventional EBS measurements, the profile of the EBS peak is mainly determined by the inverse of the disorder parameter κl_s^* (or l_s^*/λ).

2.2 *Angular Profile of Enhanced Backscattering*

Quantitatively, the angular profile of an EBS peak $I_{\mathrm{EBS}}(\theta)$ can be expressed as a 2-D Fourier transform of the radial intensity distribution of EBS[32,33]:

$$I_{\mathrm{EBS}}(q_\perp)=\int\int P(r)\exp(i\mathbf{q}_\perp\cdot\mathbf{r})d^2r, \tag{1}$$

where $\mathbf{q}_\perp$ is the projection of the wave vector onto the plane orthogonal to the backward direction ($q_\perp=2\pi\theta/\lambda$), backscattering angle θ is measured from the backscattering direction (i.e., $\theta=0$ deg corresponds to light reflected from tissue in the direction opposite to the incident light), and $P(\mathbf{r})$ is the probability of the radial intensity distribution of EBS photons with the radial vector $\mathbf{r}$ pointing from the first to the last points on a conjugated time-reversed light path ($\mathbf{r}$ is perpendicular to the incident light). If a medium is isotropic, the 2-D Fourier integral in Eq. (1) becomes:

$$I_{\mathrm{EBS}}(\theta)\propto\int_0^\infty rP(r)\exp(i2\pi r\theta/\lambda)dr. \tag{2}$$

Thus, $I_{\mathrm{EBS}}(\theta)$ is the Fourier transform of radial intensity distribution $rP(r)$. As a result, the width of an EBS peak is inversely related to that of $rP(r)$. Furthermore, from Eq. (2) one can conclude that in an EBS peak, longer light paths correspond to small scattering angles, while shorter light paths correspond to larger scattering angles.

2.3 *Principles of Low-Coherence Enhanced Backscattering*

In EBS, the conjugated time-reversed waves can interfere with each other only when they are spatially coherent, that is, the first and last points on the scattering path must be within the coherence area.[30,34] Most previous EBS measurements have been conducted using coherent laser light sources with spatial coherence length $L_{sc}\gg l_s^*$. Under such spatially coherent illumination, essentially any conjugate time-reversed waves emerging from the surface of the sample are capable of interfering with each other. However, if light incident on a sample has a finite spatial coherence length, the conjugated time-reversed waves can interfere constructively with each other only if they are spatially coherent.[34] Thus, the angular profile of an EBS intensity $I_{\mathrm{EBS}}(\theta)$ under low spatial coherence illumination can be expressed as:

$$I_{\mathrm{EBS}}(\theta)\propto\int_0^\infty C(r)rP(r)\exp(i2\pi r\theta/\lambda)dr, \tag{3}$$

where $C(r)=|2J_1(r/L_{sc})/(r/L_{sc})|$ is the degree of spatial coherence with J_1 as the first-order Bessel function.[35] As a result, the width of an LEBS peak is inversely proportional to that of the product $rP(r)C(r)$. A finite spatial coherence area acts as a spatial window rejecting long paths by preventing long traveling waves from interfering with each other. In other words, spatial coherence length limits r contributing to the EBS signal.

Incoherent waves have no correlations in phase and generate only the incoherent background intensity. If L_{sc} is sufficiently short, i.e., $L_{sc}\ll l_s^*$, low spatial coherence illumination allows only low-order scattering to give rise to the EBS peak, which in turn results in a dramatic (e.g., several orders of magnitude) broadening of an EBS peak. As discussed later, such an anomalously broad width of EBS could not be explained by simple diffusion-theory-based models of EBS.

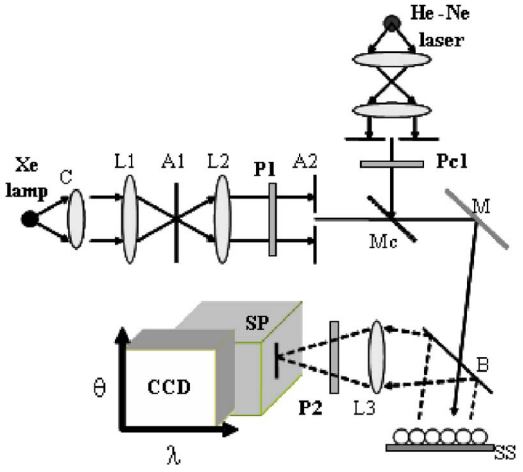

Fig. 2 LEBS spectroscopy instrument. C: condenser, L: lenses, A: apertures, P: polarizers, M: mirror, B: beamsplitter, SS: sample stage, and SP: imaging spectrograph. The entrance slit of the imaging spectrograph is in the focal plane of lens L3. Thus, all scattered light rays with an identical scattering angle θ are focused into the same point on the entrance slit. The spectrograph disperses this light in the direction perpendicular to the slit according to its wavelengths. Thus, the CCD records a matrix of scattered intensities as a function of wavelength and scattering angle $I_{\mathrm{EBS}}(\theta,\lambda)$.

3 Low-Coherence Enhanced Backscattering Spectroscopy

3.1 *Low-Coherence Enhanced Backscattering Instrument*

To overcome the limitations in conventional EBS measurements in tissue, we have recently developed low-coherence enhanced backscattering (LEBS) spectroscopy by combining EBS measurements with low spatial coherence, broadband illumination, and spectrally resolved detection.[28,30] Figure 2 il-

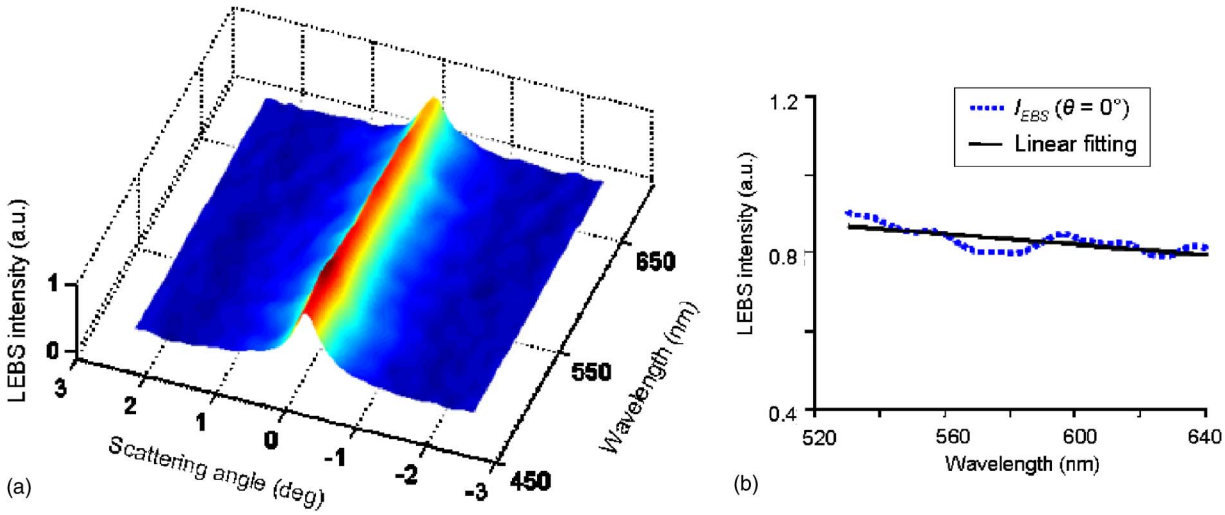

Fig. 3 (a) Representative LEBS intensity signal $I_{EBS}(\theta,\lambda)$ obtained from human colonic tissue using the LEBS spectroscopy instrument (L_{sc} =110 μm). (b) Typical LEBS intensity spectrum in the backward direction $I_{EBS}(\theta=0\ \text{deg},\lambda)$, from (a). A linear fit to $I_{EBS}(\lambda)$ using linear regression accounts for the most spectral variance of the LEBS intensity signal.

lustrates the design of an LEBS instrument. A beam of broadband cw light from a 100-W xenon lamp (Spectra-Physics Oriel Instruments, Stratford, Connecticut) was collimated using a 4-*f* lens system (divergence angle ranging from ~0.04 deg for L_{sc}=200 μm to ~0.30 deg for L_{sc}=35 μm), polarized, and delivered onto a sample at ~10 deg angle of incidence to prevent the collection of specular reflection. By changing the aperture size in the 4-*f* lens system, we varied the spatial coherence length L_{sc} of the incident light from 200 to 35 μm. The spatial coherence length was confirmed by double-slit interference experiments.[35] The light backscattered by the sample was collected by a sequence of a lens, a linear analyzer (Lambda Research Optics, Incorporated, Costa Mesa, California), and an imaging spectrograph (SpectraPro-150, Acton Research, Acton, Massachusetts). The spectrograph was positioned in the focal plane of the lens and coupled with a charge-coupled device (CCD) camera (CoolSnap HQ, Princeton Instruments Incorporated, Trenton, New Jersey). The lens projected the angular distribution of the backscattered light onto the slit of the spectrograph. Then, the imaging spectrograph dispersed this light according to its wavelength in the directions perpendicular to the slit, and projected it onto the CCD camera. Thus, the CCD camera recorded a matrix of light-scattering intensities as a function of wavelength λ and backscattering angle θ. In each CCD pixel, collected light was integrated within a certain narrow band of wavelengths around λ. The width of this band was determined by the width of the spectrograph slit. Because the temporal coherence of light L_{tc} was related to its spectral composition, finite-spectral band detection resulted in low temporal coherence detection. Accordingly, L_{tc} was dependent on the spectral resolution of the spectrograph, such that $L_{tc}=\sqrt{(2\ln 2)/\pi}\cdot(\lambda^2/\Delta\lambda)=30$ μm, where $\Delta\lambda=9$ nm is the FWHM of the detection bandpass. We also used a He-Ne laser (Melles Griot, Carlsbad, California) to compare our measurements to the conventional EBS measurements under coherent illumination.

3.2 *Characteristics of Low-Coherence Enhanced Backscattering*

3.2.1 *Spectroscopic measurements*

Using LEBS spectroscopy, EBS profiles can be observed as a function of wavelength as shown in Fig. 3(a). The design of the LEBS spectroscopy instrument enables simultaneous measurement of the spectral (λ=400 to 700 nm) and scattering angle (θ=−5 to 5 deg) distributions of backscattered light. Several spectroscopic techniques have been shown to be highly useful for tissue diagnosis and characterization including reflectance, light scattering, fluorescence, and other types of spectroscopy. Consequently, the analysis of EBS spectra may be used to provide additional information about tissue.

3.2.2 *Speckle reduction*

The experimental observation of EBS requires ensemble or configuration averaging because of speckle, which arises from random interference effects. For example, rotating the sample mechanically or averaging independent measurements are commonly used in conventional EBS measurements. Speckle becomes more severe in the absence of Brownian motion, hampering EBS studies in biological tissue.[21] However, LEBS overcomes this problem. Figure 4(a) shows the angular distribution of the backscattered light obtained from *ex vivo* human colon tissue using coherent illumination (i.e., He-Ne laser). Evidently, the speckle pattern masks an EBS peak. To uncover an EBS peak from the background of speckle, averaging over thousands of independent measurements is required. On the other hand, Fig. 4(b) shows that in the case of the LEBS signal recorded from the same tissue site, speckle is negligible and a cusp of an enhanced backscattering peak can be easily identified. Both low spatial coherence illumination and low temporal coherence detection result in speckle reduction. In our LEBS measurements, a single LEBS reading averages over multiple independent coherence volumes (each coherence volume generated an independent speckle volume). For

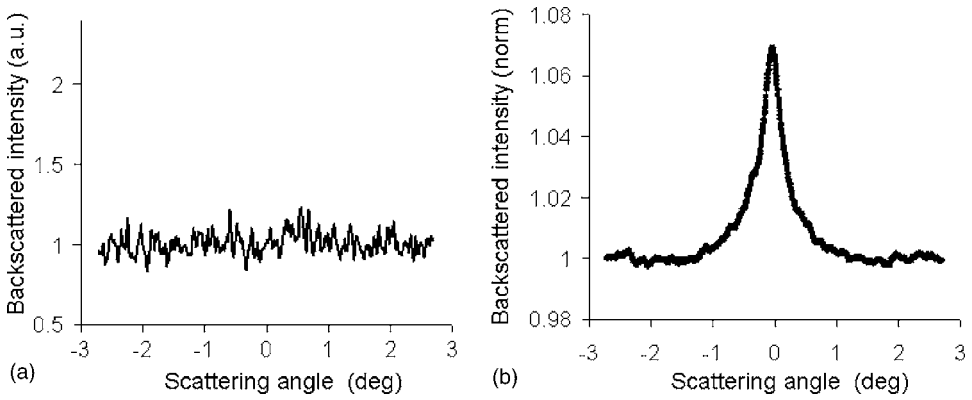

Fig. 4 LEBS enables substantial reduction of speckle. (a) The angular distribution of backscattered intensity obtained from *ex vivo* human colonic tissue using a coherent illumination (He-Ne laser, $\lambda = 632$ nm). An EBS peak is masked by severe speckle. (b) The angular profile of backscattered intensity from the identical tissue site recorded using the LEBS spectroscopy instrument (xenon lamp, $L_{sc} = 110$ μm, $\lambda = 647$ nm). A cusp of LEBS not obstructed by speckle can be clearly identified.

example, for $L_{sc} \approx 150$ μm, the number of independent coherence volumes $(D/L_{sc})^2 \times (l/L_{tc}) \approx 1000$, where D is the diameter of illumination area on the sample and l is the average path length. Therefore, LEBS measurements are easily achieved in random media, even in the absence of Brownian motion without the need for ensemble or configuration averaging.

3.2.3 *Anomalous broadening of enhanced backscattering peaks*

Broadening of EBS under low coherence illumination is perhaps the most dramatic feature of the LEBS phenomenon. It also facilitates experimental observation of LEBS. Since the width of a conventional EBS peak in general is inversely proportional to l_s^*, the width of an EBS peak in tissue and other random media with long l_s^* is extremely narrow, typically $w \approx 0.001$ deg. On the other hand, an LEBS peak is extremely broad with $w \approx 0.5$ deg, which is more than 100 times greater than the width of a conventional EBS peak expected under spatially coherent illumination. Such a dramatic increase in the LEBS peak width cannot be explained using conventional diffusion-approximation-based models of EBS, because scattering angles of photons leaving a tissue are not typically considered in modeling of conventional EBS in the diffusion regime ($L_{sc} \gg l_s^*$). Although simple substitution of $P(r)$ from the diffusion approximation into Eq. (3) predicts a broader LEBS peak, the LEBS peak observed experimentally is still nearly four times broader than that of the simple prediction from a diffusion approximation. This extra broadening of $I_{\mathrm{EBS}}(\theta)$ results from a narrower profile of $P(r)$ than that predicted by the diffusion approximation when $r < \sim l_s$ and θ is close to the backward direction.

3.2.4 *Depth-selective low-coherence enhanced backscattering measurements*

Depth-selective LEBS spectroscopy of tissue can be achieved by three means: 1. varying coherence length L_{sc}, 2. analysis of LEBS spectra $I_{\mathrm{EBS}}(\theta)$ at different scattering angles θ, and 3. analysis of the probability of the radial intensity distribution of LEBS photons $P(r)$, which can be obtained via the Fourier transform of $I_{\mathrm{EBS}}(\theta)$. In brief, L_{sc} determines the maximum penetration depth. Then, detailed depth-resolution can be obtained by either means 2 or 3.

Control of tissue depth probed with LEBS via coherence length. Only photons emerging from the tissue surface at distances $r < \sim L_{sc}$ from their point of entry into the tissue can contribute to LEBS, which limits the depth of penetration of LEBS photons to up to $\sim L_{sc}$.

Control of tissue depth probed with LEBS via the analysis of $I_{\mathrm{EBS}}(\theta)$ at different θ. As discussed before, because $I_{\mathrm{EBS}}(\theta)$ is the Fourier transform of $P(r)$, short light paths (small r) mainly give rise to the periphery of an EBS peak (large θ), while longer light paths ($r \approx L_{sc}$) give rise to the top (or center) of the EBS peak ($\theta \rightarrow 0$ deg).[29] This property of LEBS can be used to sample various depths using a single LEBS measurement by analyzing $I_{\mathrm{EBS}}(\theta)$ at different θ. Figure 5(a) shows LEBS penetration depth $L_p(\theta)$ for $l_s = 81$ μm and $l_s^* = 614$ μm. As expected, small θ correspond to deeper penetration depths, whereas large θ correspond to shorter depths. Therefore, different depths can be selectively assessed by probing a corresponding scattering angle. For example, in the case of colonic mucosa, $I_{\mathrm{EBS}}(\theta = 0.25$ deg) enables assessment of an epithelial cell layer (~ 40 μm), whereas $I_{\mathrm{EBS}}(\theta = 0$ deg) allows probing the entire mucosa (~ 70 μm).

Control of tissue depth probed with LEBS via the analysis of $P(r)$ at different r. A more precise control of tissue depth probed with LEBS can be achieved by means of the analysis of $P(r)$,[29] which in turn can be obtained from the Fourier transform of $I_{\mathrm{EBS}}(\theta)$. It is well known that the depth of penetration of photons increases with r. As shown in Fig. 5(b), tissue depths from ~ 40 μm (a single cell layer) to ~ 100 μm (thickness of colonic mucosa) can be selectively assessed by means of the analysis of $P(r, \lambda)$ by choosing appropriate parameter r. We also point out that a direct measurement of $P(r)$ for small r ($r < 300$ μm) is extremely difficult.[36]

The three means to achieve depth-selective measurements of tissue discussed before are complimentary. Thus, LEBS

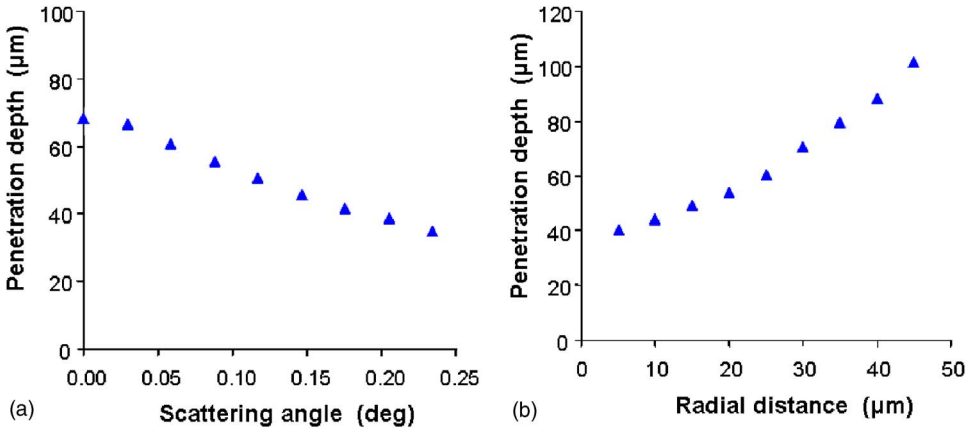

Fig. 5 (a) LEBS depth of penetration $L_p(\theta)$ as a function of θ (l_s=81 μm and l_s^*=614 μm). (θ is measured from the backscattering direction, i.e., θ=0 deg corresponds to the direction opposite to that of the incident light.) $L_p(\theta)$ decreases with θ. (b) LEBS depth of penetration $L_p(r)$ as a function of r (l_s=81 μm and l_s^*=614 μm). $L_p(r)$ increases with r. Thus, different depths of penetration can be assessed by probing different θ or r within an EBS peak (see text for details).

spectroscopy opens up the possibility of performing spectroscopic measurements at any given depth within the maximum penetration depth determined by L_{sc}.

The significance of depth-selective spectroscopic measurements for tissue characterization and diagnosis is underscored by the following reasons. 1. The most superficial tissue layer (i.e., the epithelium) is the origin of nearly 90% of human cancers and the epithelial cells are the first affected in carcinogenesis.[37] Thus, obtaining diagnostic information from most superficial tissue is crucial for the early diagnosis of epithelial precancerous lesions. 2. Hemoglobin absorption in the blood vessels located underneath the epithelium is a particularly notorious problem, as it obscures the endogenous spectral signatures of epithelial cells. 3. The depth-dependent biological heterogeneity of the epithelium underscores the need to selectively assess the epithelial cells at different depths. For example, in the colon (the major unit of organization of the mucosa is the crypt), the epithelial cells at the base of the crypt (~80 μm below the tissue surface) are capable of proliferation, while the epithelial cells at the top of the crypt (~40 μm) undergo apoptosis, as illustrated in Fig. 6. In adenomatous colonic mucosa, the apoptotic activity is reduced in the base of the crypt while the proliferative activity is increased in the lumenal surface of the colon.[38] The cells that are initially involved in neoplastic transformations are located in a specific area of the crypt: the base of the crypt is known as the location for initiation of colon carcinogenesis.[39]

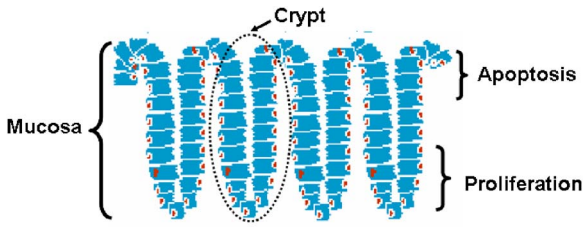

Fig. 6 The crypt: the major unit of the colonic mucosa. The epithelial cells have distinct cell activities at various depths. Typical depth of a colonic crypt is 70 to 90 μm.

Similar considerations apply to most other types of epithelia, including stratified squamous epithelium (such as the epithelium of uterine cervix, oral cavity, etc.).

4 Potential Application of Low-Coherence Enhanced Backscattering Spectroscopy for Colon Cancer Screening

4.1 *Colorectal Cancer*

Colorectal cancer (CRC) will be diagnosed in approximately 140,000 Americans this year, leading to 50,000 deaths, which makes CRC the second leading cause of cancer deaths in the United States.[40] Given that CRC is curable if diagnosed early, widespread screening has been proposed to reduce CRC fatalities. For example, colonoscopy has shown to dramatically reduce CRC fatalities through both early detection of CRC and cancer prevention. Although colonoscopy is remarkably effective in reducing CRC, screening the entire at-risk population (>60 million Americans over age 50) through colonoscopy is impossible for a variety of reasons, including expense (the cost of detection of a single colon cancer case would be >$1,000,000), patient reluctance, and complication rate. Therefore, development of novel initial-screening (risk-stratification) techniques is imperative. Many screening techniques take advantage of the "field effect" (or field cancerization) in CRC. The field effect refers to the proposition that the genetic/environmental milieu that results in a neoplastic lesion in one area of the colon also leads to alterations to tissue composition, structure, and function in the entire colon. Accordingly, detection of such changes in an easily accessible part of the colon (e.g., the rectum or sigmoid colon) can be used to infer the risk of carcinogenesis in the rest of the colon.[41] Unfortunately, the most widely used initial screening techniques such as fecal occult blood tests and flexible sigmoidoscopy (i.e., visual evaluation of the rectal and sigmoid colonic mucosa, which is the easiest to access) are suffered by low sensitivity. Thus, development of an alternative minimally invasive screening/risk-stratification test that is accurate, sensitive, cost effective, easy to perform, and does not

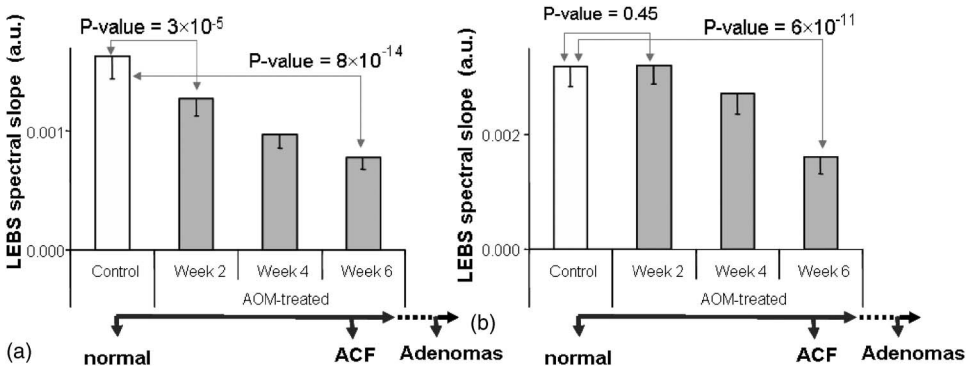

Fig. 7 LEBS spectral slopes obtained from rat colonic tissue 2, 4, and 6 weeks after the initiation of colon carcinogenesis (i.e., AOM injection) compared to those obtained from the negative control (i.e., saline-treated rats). (a) The lower compartment ($L_p \approx 70$ μm) of the crypt. (b) The upper compartment ($L_p \approx 40$ μm) of the crypts. These changes in LEBS spectra are observed in the earliest stages of colon carcinogenesis, preceding expression of currently known histological and molecular biomarkers.

require the need for colonoscopy and colon preparation is indeed crucial.

4.2 *Animal and Human Studies*

We have investigated the potential of depth-selective LEBS spectroscopy for accurate CRC risk stratification in two animal models of experimental CRC and pilot human studies.[28–31] First, we have performed animal studies with the azoxymethane (AOM)-treated rat model of colon carcinogenesis. This is one of the most robust and well-tested animal models of colon carcinogenesis.[28–30] In the AOM-treated rats, colon carcinogenesis progresses through the same steps as in humans: the earliest detectable marker of colon carcinogenesis, aberrant crypt foci (ACF) develop 8 to 12 weeks after the AOM injection, adenomas are observed in 20 to 30 weeks, and carcinomas develop in 40 weeks. 48 male Fisher 344 rats (150 to 200 g) (Sigma, Saint Louis, Missouri) were randomized to two weekly intraperitoneal (i.p.) injections with either AOM (15 mg/kg) or saline (in the case of negative control animals). Animals were euthanized at specified time points (2, 4, and 6 weeks after the second AOM injection). Colons were removed, opened longitudinally, and washed. LEBS measurements were performed on fresh, unfixed colons within one hour of sacrifice. We recorded LEBS signals from at least 20 tissue sites per animal equally distributed throughout colonic surfaces. Moreover, to ensure that our findings are not model specific, we used male multiple intestinal neoplasia (MIN) (Jackson Laboratory, Bar Harbor, Maine) and control C57BL6 mice (wildtype at the adenomatous polyposis coli locus) at 6 to 7 weeks of age ($n=18$).[31] In the MIN model, adenomatous polyposis coli (APC) truncation leads to spontaneous intestinal tumorigenesis, thus replicating the human familial adenomatous polyposis. The MIN mice develop intestinal adenomas at 9 to 10 weeks of age, and most intestinal adenomas occur in the small intestine. We point out that the time points for which we have recorded LEBS signals (i.e., 2 to 6 weeks after AOM injection in the case of the AOM animal model and 6 to 7 week old mice in the case of the MIN mice model) correspond to very early stages of carcinogensis. At these early time points, no currently known histologic, molecular, or genetic markers have been able to detect preneoplastic transformation. Finally, to investigate whether our findings in these animal models can be translated into humans, we performed human studies of 63 subjects undergoing colonoscopy.[31] We used six biopsies of endoscopically normal mucosa at least 3 cm away from any neoplastic lesion to validate whether LEBS spectroscopy can be used to detect the field effect of CRC. In the human studies, we defined a low-risk group as subjects without personal history of neoplasia and family history of adenomas or carcinomas, and a high-risk group ($n=12$) as subject with adenomas on current colonoscopy (all adenomas were histologically confirmed), respectively.

4.3 *Results*

We identified the optimal depth of penetration for which LEBS markers are the most diagnostic. We assessed LEBS spectra corresponding to 30-, 50-, and 70-μm depths ($\theta=0.4$ deg, $\theta=0.2$ deg, and $\theta=0$ deg, respectively) and found that 70-μm penetration depth provides the most diagnostically significant results and enables detection of CRC at the earliest time point (2 weeks after AOM injection).[31] It is of notice that this depth approximately corresponds to the depth of colonic mucosa, and several lines of evidence suggest that the base of the crypt is the location for initiation of colon carcinogenesis.

Typically, $I_{\mathrm{EBS}}(\lambda)$ is a declining function of wavelength and its steepness depends on the size distribution of submicron intraepithelial structures.[42] Although LEBS spectra are quite complex with the scale of spectral features as small as only a few nanometers, a linear fit to $I_{\mathrm{EBS}}(\lambda)$ using linear regression from 530 to 640 nm accounts for the most spectral variance. For example, Fig. 3(b) shows a typical $I_{\mathrm{EBS}}(\lambda, \theta=0 \text{ deg})$ recorded from a human colon tissue and its linear fit with $R^2 \approx 0.6$. Thus, to characterize the spectrum of $I_{\mathrm{EBS}}(\lambda)$ as a biomarker, we obtained the value of the slope of the fit over wavelength, which is referred to as the LEBS spectral slope. We found that the LEBS spectral slope showed excellent temporal and spatial correlations with the progression of carcinogenesis in the animal models and the pilot human studies. Figures 7(a) and 7(b) show alterations of LEBS spectral slope obtained from the AOM-treated rats compared with control values in the two different compartments. As shown in

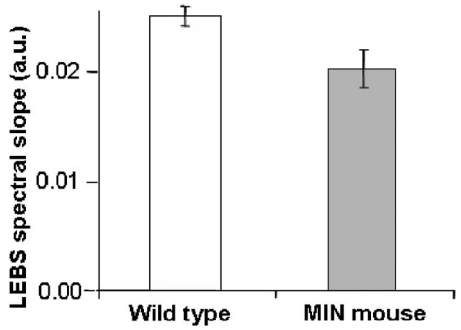

Fig. 8 LEBS spectral changes confirmed in the MIN mouse model of intestinal carcinogenesis. LEBS spectral slope obtained from the microscopically normal appearing (i.e., uninvolved) intestinal mucosa in 6-week-old MIN mice is significantly different from one obtained from age-matched control mice (wild type) ($L_p \approx 70$ μm).

Fig. 7(a), spectral slope of the basal compartment is dramatically decreased as early as 2 weeks after the AOM administration, and decreases over the process of carcinogenesis. On the other hand, LEBS spectral slope of the lumenal compartment remains unchanged at the 2-week time point but instead changes dramatically later in the time course of the experiment. These results show that the LEBS spectral slope from ~70-μm depth provides the earliest sensitivity between the saline-treated rats and the AOM-treated rats. We also confirmed this result in the 6-week-old MIN mice. As shown in Fig. 8, the LEBS spectral slope is diagnostic for the early preadenoma stage of intestinal neoplasia in histologically normal mucosa of MIN mice (P value=0.009).

Furthermore, we found that the change in the LEBS spectral slope is also diagnostic in humans. This is illustrated in Fig. 9, which shows a significant decrease in the spectral slope obtained from the colonoscopically normal rectal mucosa in patients who harbored adenomas elsewhere in the colon when compared to those who were neoplasia free (P value=0.006). Adenomas were approximately equally distributed between the sigmoid colon/rectum (28% of all adenomas), transverse colon (35%), and the cecum (38%). The

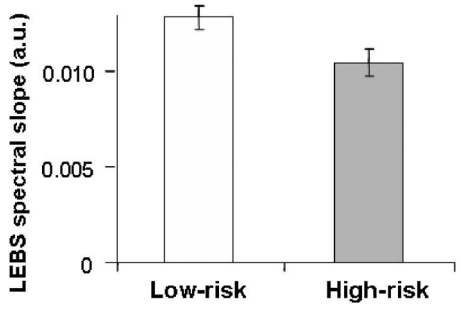

Fig. 9 Pilot human studies. LEBS spectral changes have the potential to diagnose colonic neoplasia in humans without the need for colonoscopy. LEBS spectral slope assessed in the rectum of subjects undergoing colonoscopy ($L_p \approx 70$ μm) correlates with presence of neoplasia elsewhere in the colon (P value=0.006). High-risk groups include subjects with advanced adenomas anywhere in the colon (cecal, colonic, or rectal adenoma >10 mm), while low-risk groups (i.e., no dysplasia) include patients without personal or family history of colonic neoplasia.

magnitude of decrease in LEBS spectral slope appeared to be greater if the lesion was located in the proximity to the site of LEBS analysis. However, significant differences were noted from LEBS measurements taken at distant sites as well (e.g., rectal LEBS spectral slope correlates with the presence of adenomas in the transverse colon). These results demonstrate that LEBS spectroscopy has the potential to accurately risk-stratify patients for CRC and may be translated into a practical clinical method for colon cancer screening. Translation of LEBS into clinical practice will require development of fiber optics LEBS probes that can be used to record LEBS spectra from rectal mucosa *in vivo* and assess LEBS markers without the need for colonoscopy or biopsy. The development of such LEBS fiber optics probes is currently underway in our research group. Rectal LEBS tests can potentially be performed without the need for colonoscopy or patients' colonic preparation. We envision that in the future the LEBS technique may enable a primary care physician to assess LEBS biomarkers during a patient's annual physical exam and thus determine the risk of CRC and the need for colonoscopy.

5 Discussion

LEBS possess two unique features compared to the majority of other conventional spectroscopic techniques such as 4-D elastic light scattering fingerprinting[42] and polarized light scattering spectroscopy. 1. LEBS has the capability to probe a specific depth within the maximal depth determined by the spatial coherence length of illumination. The ability to assess epithelial cells is critical to study human cancers, because most human cancers originate from epithelial cells, resulting from a series of pathologic changes that transform normal epithelium into invasive carcinoma. One important criterion for bioassays of carcinogenesis is the use of epithelial cells. The significance of the depth selectivity of LEBS is further underscored by the need to selectively assess epithelial cells at different tissue depths. For example, colonic epithelial cells have distinct function, depending on their depth. In particular, epithelial cells at the base of the crypt are capable of proliferation, whereas epithelial cells at the top of the crypt undergo apoptosis. As our data demonstrate, selective targeting of specific depths within colonic epithelium provides improved accuracy in the diagnosis of epithelial precancers compared to the spectroscopic analysis of unpolarized or linearly polarized light that does not differentiate epithelial and stromal layers. 2. LEBS offers a unique contrast for tissue assessment—double scattering—whereas other conventional spectroscopic techniques are based either on single scattering or diffuse reflectance. Double scattering is the minimal scattering events that are required to generate an EBS peak in discrete random media,[15,43] because single scattering can only generate the incoherent baseline backscattering signal but not to EBS. Because biological tissue is a weakly scattering random medium with transport mean path length on the order of millimeters ($l_s^* \gg L_{sc}$), the small spatial coherence area, which dephases the time-reversed paths outside its coherence areas, can isolate the minimal number of scattering events (i.e., double scattering) in EBS.[44] Thus, LEBS originates mainly from the conjugated time-reversed paths of double scattering events in biological tissue. In other words, the most probable scattering event of LEBS in biological tissue is double scattering. Such

unique features of LEBS will further facilitate the utilization of LEBS for tissue characterization and diagnosis among other currently used optical spectroscopic techniques.

6 Conclusion

We demonstrate that LEBS is an ideal tool to exploit the EBS phenomenon in biological tissue and other random media with long transport mean free paths. LEBS overcomes all major hurdles so far preventing the use of EBS in tissue optics. The use of low-coherence illumination has several important implications on LEBS, including dramatic broadening of the angular profile of an LEBS peak and substantial speckle reduction. Moreover, LEBS enables depth-selective spectroscopic assessment of tissue. The LEBS signal originates primarily from double scattering of light in tissue. Thus, LEBS provides unique information about tissue compared to other existing spectroscopic techniques that are based either on single scattering or diffuse reflectance. Furthermore, we demonstrate that LEBS spectroscopy has potential applications for tissue diagnosis. Specifically, we show that LEBS may enable detection of colon carcinogenesis earlier than other existing histological or molecular techniques, and may potentially enable colon cancer screening without the need for colonoscopy and colon preparation. We believe that LEBS could potentially be of benefit to clinicians developing effective anticancer strategies, to pharmaceutical companies developing or evaluating anticancer agents, and to biomedical researchers investigating the mechanisms of carcinogenesis.

Acknowledgments

The study was supported by National Institutes of Health (NIH) grants R01 EB003682 and R01 CA112315, National Science Foundation (NSF) grant BES-0238903, and a grant from The Wallace H. Coulter Foundation. Y.L. Kim was supported in part by a National Cancer Institute training grant R25 CA100600–01A1.

References

1. M. P. van Albada and A. Lagendijk, "Observation of weak localization of light in a random medium," *Phys. Rev. Lett.* **55**(24), 2692–2695 (1985).
2. P. E. Wolf and G. Maret, "Weak localization and coherent backscattering of photons in disordered media," *Phys. Rev. Lett.* **55**(24), 2696–2699 (1985).
3. Y. Kuga and A. Ishimaru, "Retroreflectance from a dense distribution of spherical-particles," *J. Opt. Soc. Am. A Opt. Image Sci. Vis* **1**(8), 831–835 (1984).
4. D. S. Wiersma, M. P. Vanalbada, B. A. Vantiggelen, and A. Lagendijk, "Experimental-evidence for recurrent multiple-scattering events of light in disordered media," *Phys. Rev. Lett.* **74**(21), 4193–4196 (1995).
5. G. Labeyrie, F. de Tomasi, J. C. Bernard, C. A. Muller, C. Miniatura, and R. Kaiser, "Coherent backscattering of light by cold atoms," *Phys. Rev. Lett.* **83**(25), 5266–5269 (1999).
6. R. Sapienza, S. Mujumdar, C. Cheung, A. G. Yodh, and D. Wiersma, "Anisotropic weak localization of light," *Phys. Rev. Lett.* **92**(3), 033903 (2004).
7. J. Huang, N. Eradat, M. E. Raikh, Z. V. Vardeny, A. A. Zakhidov, and R. H. Baughman, "Anomalous coherent backscattering of light from opal photonic crystals," *Phys. Rev. Lett.* **86**(21), 4815–4818 (2001).
8. D. S. Wiersma, M. P. van Albada, and A. Lagendijk, "Coherent backscattering of light from amplifying random-media," *Phys. Rev. Lett.* **75**(9), 1739–1742 (1995).
9. P. C. de Oliveira, A. E. Perkins, and N. M. Lawandy, "Coherent backscattering from high-gain scattering media," *Opt. Lett.* **21**(20), 1685–1687 (1996).
10. M. I. Mishchenko and J. M. Dlugach, "Coherent backscatter and the opposition effect for E-type asteroids," *Planet. Space Sci.* **41**(3), 173–181 (1993).
11. R. Vreeker, M. P. van Albada, R. Sprik, and A. Lagendijk, "Femtosecond timeresolved measurements of weak localization of light," *Phys. Lett. A* **132**(1), 51–54 (1988).
12. K. M. Yoo, Y. Takiguchi, and R. R. Alfano, "Weak localization of photons: contributions from the different scattering pathlengths," *IEEE Photonics Technol. Lett.* **58**, 94–96 (1989).
13. A. Wax, S. Bali, and J. E. Thomas, "Time-resolved phase-space distributions for light backscattered from it disordered medium," *Phys. Rev. Lett.* **85**(1), 66–69 (2000).
14. S. Etemad, R. Thompson, and M. J. Andrejco, "Weak localization of photons—Termination of coherent random-walks by absorption and confined geometry," *Phys. Rev. Lett.* **59**(13), 1420–1423 (1987).
15. M. B. van der Mark, M. P. van Albada, and A. Lagendijk, "Light-scattering in strongly scattering media—Multiple-scattering and weak localization," *Phys. Rev. B* **37**(7), 3575–3592 (1988).
16. F. C. Mackintosh and S. John, "Coherent backscattering of light in the presence of time-reversal-noninvariant and parity-nonconserving media," *Phys. Rev. B* **37**(4), 1884–1897 (1988).
17. R. Lenke, R. Lehner, and G. Maret, "Magnetic-field effects on coherent backscattering of light in case of Mie spheres," *Europhys. Lett.* **52**(6), 620–626 (2000).
18. C. Schwartz and A. Dogariu, "Enhanced backscattering of optical vortex fields," *Opt. Lett.* **30**(12), 1431–1433 (2005).
19. K. M. Yoo, F. Liu, and R. R. Alfano, "Biological-materials probed by the temporal and angular profiles of the backscattered ultrafast laser-pulses," *J. Opt. Soc. Am. B* **7**(8), 1685–1693 (1990).
20. K. M. Yoo, G. C. Tang, and R. R. Alfano, "Coherent backscattering of light from biological tissues," *Appl. Opt.* **29**(22), 3237–3239 (1990).
21. G. Yoon, D. N. G. Roy, and R. C. Straight, "Coherent backscattering in biological media—Measurement and estimation of optical-properties," *Appl. Opt.* **32**(4), 580–585 (1993).
22. J. F. Beek, P. Blokland, P. Posthumus, M. Aalders, J. W. Pickering, H. Sterenborg, and M. J. C. van Gemert, "*In vitro* double-integrating-sphere optical properties of tissues between 630 and 1064 nm," *Phys. Med. Biol.* **42**(11), 2255–2261 (1997).
23. T. J. Farrell, M. S. Patterson, and B. Wilson, "A diffusion-theory model of spatially resolved, steady-state diffuse reflectance for the noninvasive determination of tissue optical-properties *in vivo*," *Med. Phys.* **19**(4), 879–888 (1992).
24. A. Z. Genack, "Optical-transmission in disordered media," *Phys. Rev. Lett.* **58**(20), 2043–2046 (1987).
25. S. A. Prahl, M. J. C. Vangemert, and A. J. Welch, "Determining the optical-properties of turbid media by using the adding-doubling method," *Appl. Opt.* **32**(4), 559–568 (1993).
26. S. Etemad, R. Thompson, and M. J. Andrejco, "Weak localization of photons—universal fluctuations and ensemble averaging," *Phys. Rev. Lett.* **57**(5), 575–578 (1986).
27. M. Tomita and H. Ikari, "Influence of finite coherence length of incoming light on enhanced backscattering," *Phys. Rev. B* **43**(4), 3716–3719 (1991).
28. Y. L. Kim, Y. Liu, R. K. Wali, H. K. Roy, and V. Backman, "Low-coherent backscattering spectroscopy for tissue characterization," *Appl. Opt.* **44**(3), 366–377 (2005).
29. Y. L. Kim, Y. Liu, V. M. Turzhitsky, R. K. Wali, H. K. Roy, and V. Backman, "Depth-resolved low-coherence enhanced backscattering," *Opt. Lett.* **30**(7), 741–743 (2005).
30. Y. L. Kim, Y. Liu, V. M. Turzhitsky, H. K. Roy, R. K. Wali, and V. Backman, "Coherent backscattering spectroscopy," *Opt. Lett.* **29**(16), 1906–1908 (2004).
31. H. K. Roy, Y. L. Kim, Y. Liu, R. K. Wali, M. J. Goldberg, V. M. Turzhitsky, J. Horwitz, and V. Backman, "Colon carcinogenesis risk-stratification through enhanced backscattering spectroscopy (EBS) analysis of the uninvolved colonic mucosa," *Clin. Cancer Res.* **12**(3), 961–968 (2006).
32. P. E. Wolf, G. Maret, E. Akkermans, and R. Maynard, "Optical coherent backscattering by random-media—an experimental-study," *J. Phys. (France)* **49**(1), 63–75 (1988).

33. M. Ospeck and S. Fraden, "Influence of Reflecting Boundaries and Finite Interfacial Thickness on the Coherent Backscattering Cone," *Phys. Rev. E* **49**(5), 4578–4589 (1994).
34. T. Okamoto and T. Asakura, "Enhanced backscattering of partially coherent light," *Opt. Lett.* **21**(6), 369–371 (1996).
35. M. Born and E. Wolf, *Principles of Optics: Electromagnetic Theory of Propagation, Interference and Diffraction of Light*, 7th ed., pp. 572–580, Cambridge University Press, Cambridge, New York (1999).
36. M. Dogariu and T. Asakura, "Reflectance properties of finite-size turbid media," *Waves Random Media* **4**(4), 429–439 (1994).
37. K. W. Kinzler and B. Vogelstein, "Colorectal tumors," in *The Genetic Basis of Human Cancer*, B. Vogelstein and K. W. Kinzler, Eds., pp. 565–587, McGraw-Hill, New York (1998).
38. A. J. M. Watson, "The role of apoptosis in intestinal disease," *J. Gastroenterol.* **32**(3), 414–423 (1997).
39. M. Brittan and N. A. Wright, "Stem cell in gastrointestinal structure and neoplastic development," *Gut* **53**(6), 899–910 (2004).
40. A. Jemal, R. C. Tiwari, T. Murray, A. Ghafoor, A. Samuels, E. Ward, E. J. Feuer, and M. J. Thun, "Cancer statistics, 2004," *Ca-Cancer J. Clin.* **54**(1), 8–29 (2004).
41. B. J. M. Braakhuis, M. P. Tabor, J. A. Kummer, C. R. Leemans, and R. H. Brakenhoff, "A genetic explanation of Slaughter's concept of field cancerization: Evidence and clinical implications," *Cancer Res.* **63**(8), 1727–1730 (2003).
42. H. K. Roy, Y. Liu, R. K. Wali, Y. L. Kim, A. K. Kromin, M. J. Goldberg, and V. Backman, "Four-dimensional elastic light-scattering fingerprints as preneoplastic markers in the rat model of colon carcinogenesis," *Gastroenterology* **126**, 1071–1081 (2004).
43. E. Akkermans, P. E. Wolf, R. Maynard, and G. Maret, "Theoretical-study of the coherent backscattering of light by disordered media," *J. Phys. (France)* **49**(1), 77–98 (1988).
44. Y. L. Kim, P. Pradhan, H. Subramanian, Y. Liu, M. H. Kim, and V. Backman, "Origin of low-coherence enhanced backscattering," *Opt. Lett.* **31**(10), 1459–1461 (2006).